Hacia los 130 años de creación de la Universidad del Zulia

"Buscar la verdad y afianzar los valores transcendentales", misión de las universidades en su artículo primero, inspirado en los principios humanísticos. Ley de Universidades 8 de septiembre de 1970.

REVISTA TÉCNICA
DE LA FACULTAD DE INGENIERÍA

Una Revista Internacional Arbitrada
que está indizada en las publicaciones
de referencia y comentarios:

- SCOPUS
- Compendex
- Chemical Abstracts
- Metal Abstracts
- World Aluminium Abstracts
- Mathematical Reviews
- Petroleum Abstracts
- Current Mathematical Publications
- MathSci
- Revencyt
- Materials Information
- Periódica
- Actualidad Iberoamericana

UNIVERSIDAD DEL ZULIA

REVISTA TÉCNICA
DE LA FACULTAD DE INGENIERÍA

Gas-Phase Thermolysis of Ethyl Chlorooxoacetate: Comparison with Ethyl Oxoacetate and Static System Details for Kinetic Study

Andreína Alexandra Reyes Yanes (iD)

Universidad Nacional Mayor de San Marcos, Facultad de Química e Ingeniería Química, Departamento Académico de Fisicoquímica. Ciudad Universitaria- Pabellón B- Calle Germán Amezaga Nº 375- Lima- Perú 15081. areyesy@unmsm.edu.pe
https://doi.org/10.22209/rt.v43n3a01
Received: 03/03/2020 | Accepted: 05/06/2020 | Available: 01/09/2020

Abstract

The advantage offered by kinetic studies in the gas phase is that the velocity coefficient is not affected by surfaces, catalysts or solvents that interact with the substrate. So far, gas phase thermolysis of esters derived from oxalic acid have been scarcely studied. In this investigation, the kinetic study of the thermal decomposition of ethyl chlorooxoacetate between 543–593 K and 76–209 mbar was carried out, using a static vacuum system whose operation are widely described. Total pressure measurements and chromatographic products analysis indicates consecutive first order reactions, unimolecular and homogeneous for substrate decarbonylation, followed by ethylene elimination, unlike the ethyl oxoacetate thermolysis, which proceeds by parallel decarboxylation and decarbonylation pathways. Arrhenius equation for the reaction studied between 543.2 – 593.1 K was found to be $\log k_1 = (13.22 \pm 0.45) - (179.4 \pm 4.9)$ kJ mol^{-1} (2.303RT)$^{-1}$ and velocity coefficient at 623 K significantly larger than for the decarbonylation of ethyl oxoacetate, suggesting that chlorine substituent would have a greater tendency than hydrogen to migrate to the adjacent carbonyl, forming more rigid bonds transition state.

Keywords: thermolysis; gas-phase kinetics; decarbonilation

Termólisis de Clorooxoacetato de Etilo en Fase Gas: Comparación con Oxoacetato de Etilo y Detalles del Sistema Estático para el Estudio Cinético

Resumen

La ventaja de los estudios cinéticos en fase gas es que el coeficiente de velocidad no es afectado por superficies, catalizadores ni disolventes que interactúen con el sustrato. La termólisis en fase gas de los ésteres derivados del ácido oxálico ha sido poco estudiada. En esta investigación se realizó el estudio cinético de la descomposición térmica de clorooxoacetato de etilo entre 543–593 K y 76–209 mbar, utilizando un sistema estático de vacío cuyo funcionamiento se describe ampliamente. Mediciones de presión total y análisis cromatográfico de productos indican reacciones consecutivas de orden uno, unimoleculares y homogéneas, de decarbonilación del sustrato seguida de la eliminación de etileno, a diferencia de la termólisis de oxoacetato de etilo, que procede por vías paralelas de decarboxilación y decarbonilación. La ecuación de Arrhenius para la reacción estudiada entre 543,2 – 593,1 K resultó ser $\log k_1 = (13,22 \pm 0,45) - (179,4 \pm 4,9)$ kJ mol^{-1} (2,303RT)$^{-1}$, y el coeficiente de velocidad a 623 K significativamente mayor que para la decarbonilación del oxoacetato de etilo sugiere que el sustituyente cloro tendría mayor disposición que el hidrógeno de migrar al carbonilo adyacente, formando un estado de transición con enlaces más rígidos.

Palabras clave: termólisis; cinética en fase gas; clorooxoacetato de etilo

Introduction

Homogeneous reactions can take place in the gas and solution phase. In the latter, there is a high probability that solvents, like surfaces and catalyst, may interact with the substrate and affect the rate coefficient. For this reason, gas-phase reactions do not constrain the use of quantum mechanical models for estimating the kinetic parameters and for studying the behavior of the isolated molecule in the transition state. However, even though gas-phase thermolysis are important for being a rare case of order one reactions and, additionally, for clarifying the structure-reactivity relationship on certain substrates under study [1-9], the number of elementary gas-phase reactions is relatively small [10]. Oxalic acid analogs have been scarcely investigated in gas phase. A theoretical-experimental study on methyl chlorooxoacetate [11] suggests the following mechanism, sustained by the agreement of the values calculated by semi-empirical methods PM3 and *ab initio* MP2/6-31G* with the experimental results at 573 K:
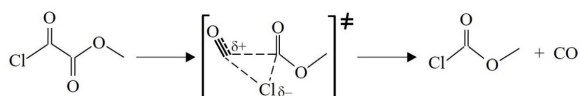

Figure 1. Methyl chlorooxoacetate thermolysis at 573 K.

The static method implies a closed reactor system to measure the total pressure of the gas generated as the reaction advances at constant volume, combined with the chemical analysis of the products at working temperature. In light of these considerations, this study aims at describing the static system for estimating the kinetic and thermodynamic parameters of ethyl chlorooxoacetate thermolysis in order to suggest a mechanism for this reaction and to make a comparison with what has been reported on ethyl oxoacetate [12], another ester derivative of oxalic acid.

Experimental

Vacuum line. It is manufactured with Pyrex glass and contains a Pyrex glass cylindrical reactor (Figure 2). The reactor remains inside an oven with controlled temperature and attached to the manometer and to the glass membrane that is responsive to changes in pressure. The products are collected in Pyrex-glass traps at liquid nitrogen temperature. The system is coupled with a rotating vacuum pump HITACHI LTD 3VP-C2, with air flow rate of 50 L min^{-1}, that generates a vacuum of 6.67×10^{-4} mbar. It also includes a mercury diffusion pump of 150 W in order to provide additional vacuum.
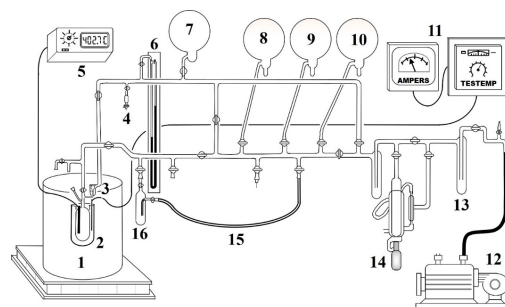

Figure 2. Static vacuum system. 1, oven. 2, reactor. 3, glass membrane. 4, relief valve. 5, digital multimeter. 6, mercury manometer. 7, schlenk flask. 8-10, CO_2, propylene and ethylene containers, respectively. 11, temperature controller. 12, vacuum pump. 13, trap for collecting gas product. 14, mercury diffusion pump. 15, rubber hose. 16, trap for collecting product for analysis.

Glass membrane. Light reflecting glass surface of 0.5 thick, coated with a thin layer of aluminum, inserted in the diaphragm and connected by a capillary tube to the reactor at its lower end and to the manometer at its upper end (Figure 3). It is lit by a lamp that produces reflection of an indicator line, which allows to establish an equilibrium point before the reaction starts. This relative zero corresponds to pressure equality on both sides of the membrane. An increase of pressure in the system due to thermolysis causes membrane deformation and sets in motion the indicator line with respect to the equilibrium point. This is measured by introducing air at the upper end of the membrane with the help of the relief valve until the indicator line is back to the reference position, and thus the manometric height reached is equivalent to the reactor total internal pressure.
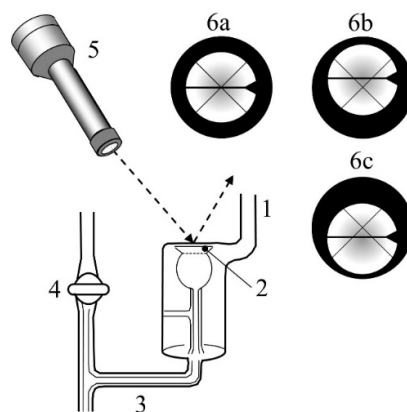

Figure 3. Optical system. 1, manometer connection. 2, glass membrane. 3, capillary tube. 4, reactor stopcock. 5, lamp. 6, display with indicator line: a, in equilibrium; b, with an increase in the reactor pressure; c, in vacuum.

Oven with temperature controller. It contains the reactor and is covered by a heating jacket of 200 V and 800 W (Figure 4), fixed on refractory bricks. Its maximum temperature variation is ± 0.2 K and it stays constant thanks to an OMEGA SSR240AC45 controller, coupled to an iron-constantan thermocouple and inserted into a whole inside the metallic block. The working temperature is measured with an iron-constantan thermocouple connected to the digital multimeter.
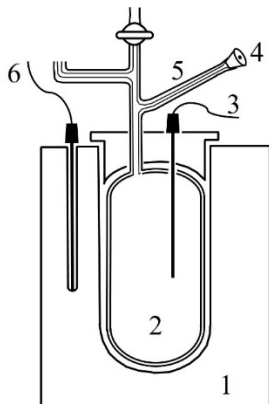

Figure 4. Longitudinal Cross section of the oven. 1, metallic block. 2, reactor. 3, thermocouple. 4, injection point with a silicone cap. 5, capillary tube. 6, thermocouple.

Calculation of kinetic data

The measures were carried out within a range of 543–593 K and 76–209 mbar. After creating a vacuum in the system, the stopcock is closed to isolate the reactor. Approximately 0.20 mL of substrate were injected to the reactor with a PERFEKTUM® syringe through the silicone cap. The pressure increment generated by gaseous products in the reactor is measured at appropriate time intervals. The substrate initial pressure in the reactor P0 is determined by extrapolation to zero time of a total pressure curve as a function of time. When additives, such as free inhibitors and standard radicals, are required, they are injected first; then, the reactor pressure is balanced and the substrate is injected next. Products undertake a gas or liquid phase chromatographic analysis at room temperature, depending of their physical state. When the necessary extent of reaction is reached, products are extracted from the reaction camera and condensed using liquid nitrogen in the PYREX glass traps connected to the vacuum system, from which air has been previously extracted. Once room temperature is reached, each sample is injected to the chromatograph until reproducible results are obtained.

Substrate characterization

The ethyl chlorooxoacetate identification (Acros

Organics, CAS Nº 4755-77-5), which was 98% pure, was verified by GC/MS [12].

Reaction products characterization

Gas-phase chromatographic analysis. The produced ethyl was quantified in a VARIAN 3700 GC gas chromatograph coupled with a VARIAN 4400 integrator with a detector FID (15 mL min^{-1} H$_2$ and 120 mL min^{-1}air) and a column packed with PORAPAK Q 80/100 mesh (3.1 m long), with N$_2$ (30 mL min^{-1}) and propylene (Matheson, Gas Products, Inc.) as carrier gas and internal standard, respectively. The oven temperature was 373 K, and the equation obtained from the calibration curve was the following:

$$P_{ethylene}/P_{propylene} = 1.556(A_{ethylene}/A_{propylene}) - 0.045 \quad (1)$$

Liquid-phase chromatographic analysis. Ethyl chloroformate, main thermolysis product observed, was analyzed with a HEWLETT- PACKARD 5710-A chromatograph coupled with HP 3392-A integrator and equipped with detector FID (30 mL min^{-1} H$_2$ and 240 mL min^{-1} air), with column packed with 10% SP 1200, 1% H$_3$PO$_4$, Chrom WAW 80/100 mesh (2 m long), the oven temperature being 313 K, with N$_2$ as carrier gas (30 mL min^{-1}) and acetone p.a. (Merck, CAS Nº 67-64-1) as internal standard. The following equation was obtained from calibration curve:

$$P_{ClCOCOOEt}/P_{acetone} = 1.556(A_{ClCOCOOEt}/A_{acetone}) - 0.045 \quad (2)$$

Calculation of rate coefficient

Ethylene, CO$_2$ and ClCOOC$_2$H$_5$ were identified among the reaction products, which suggests that they could be involved in the following reaction routes:
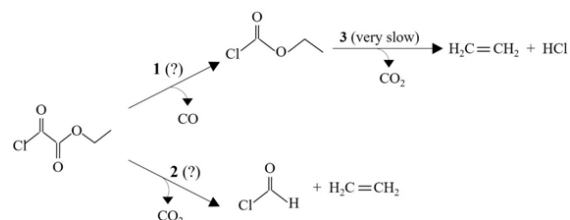

Figure 5. Possible thermal decomposition routes for ethyl chlorooxoacetate.

The rate coefficient reported for the ClCOOC$_2$H$_5$ thermolysis [13] results from the following equation for 559 - 626 K:

$$k_{ClCOCOOEt}(s^{-1}) = 1012.64\, e^{-183600\, J/8.314\, T(K)} \quad (3)$$

One verification alternative for the occurrence of all the reactions shown in Figure 5 in the working temperature range (543–593 K) is to determine the

pressure of the ethylene produced and then compare it to the one calculated for the hypothetical reaction **3**. If they are equal, only one route occurs: substrate decarbonylation, 1, whose reaction intermediary generates ethylene upon decomposition. If the calculated ethylene pressure by chromatographic analysis is higher than the one of the ethylene resulting from $ClCOOC_2H_5$ pyrolysis, it means that two parallel reactions are taking place and the remaining ethylene was generated from decarboxylation, 2. The following expression allows to determine the pressure of ethylene produced by $ClCOOC_2H_5$ pyrolysis at any time t, being residual $ClCOOC_2H_5$ pressure obtained from equation (2).

$$P_{ethylene\ generated\ from\ ClCOOEt} = P_{ClCOOEt\ residual} \left(\frac{1 - e^{k_{ClCOOEt}\ t}}{e^{k_{ClCOOEt}\ t}} \right) (4)$$

Results and Discussion

Stoichiometry. The products shown in Figure 5 were found throughout the working temperature range. CO cannot be liquified at liquid nitrogen temperature, so it was detected with a high-voltage generator [12]. Table 1 shows a comparison of theoretical results obtained from equation (4) for the expected pressure of ethylene from $ClCOOC_2H_5$ thermolysis, with the actual ethylene pressure obtained from equation (1). The difference between these values at the respective reaction times for each temperature indicates that ethylene identified in fact originates from $ClCOOC_2H_5$ decomposition and a parallel decarboxylation reaction does not occur as in ethyl oxoacetate thermolysis.

Table 1. Comparison between total ethylene analyzed in ethyl chlorooxoacetate thermolysis and ethylene generated by ethyl chloroformate thermolysis at different temperatures.

T (K)	Parameter	Value		
	t (min)	20	30	40
563.2	$P_{ethylene,\ GC}$ (mbar)	0.19	0.29	0.27
	$P_{ethylene\ generated\ from\ ClCOOEt}$ (mbar)	2.00	2.93	3.60
	t (min)	12	15	20
573.2	$P_{ethylene,\ GC}$ (mbar)	2.53	3.07	3.73
	$P_{ethylene\ generated\ from\ ClCOOEt}$ (mbar)	2.40	2.93	3.87
	t (min)	2	3	6
593.1	$P_{ethylene,\ GC}$ (mbar)	0.67	1.47	3.73
	$P_{ethylene\ generated\ from\ ClCOOEt}$ (mbar)	0.80	1.60	4.00

The produced ethylene pressure is low because $ClCOOC_2H_5$ thermolysis in the working range is very slow. On the other hand, even though the HCl analysis was not carried out, it was possible to detect the presence of CO in the vacuum line. Based on these observations, the following sequence of reactions for ethyl chlorooxoacetate thermal decomposition may be suggested:
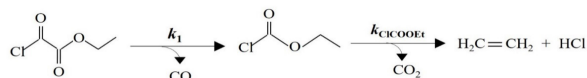

Figure 6. Reactions identified for ethyl chlorooxoacetate pyrolysis.

The similarity of reaction percentage yield determined through the different methods is evident in Table 2, which supports the stoichiometry proposed. For each reaction time, they were obtained from the following equations, where P_0 is substrate initial pressure within the reactor:

$$\text{Reaction percent yield (manometric method)} = 100[(P_{total}/P_0) - 1] \quad (5)$$

$$\text{Reaction percent yield (cromatographic method)} = 100[(P_{ClCOCOOEt}/P_0)] \quad (6)$$

Table 2. Stoichiometry verification for ethyl chlorooxoacetate thermolysis at 573.2 K.

Parameter	Value				
t (min)	7	10	12	15	20
Reaction percent yield (chromatographic method)	26.2	33.5	41.0	46.8	54.8
Reaction percent yield (manometric method)	26.9	34.6	40.4	46.8	56.4

Reaction order. The linear correlation shown in Figure 7 suggests a first-order kinetics throughout the working temperature range, like the first-order decarbonylation reaction in ethyl oxoacetate thermolysis.
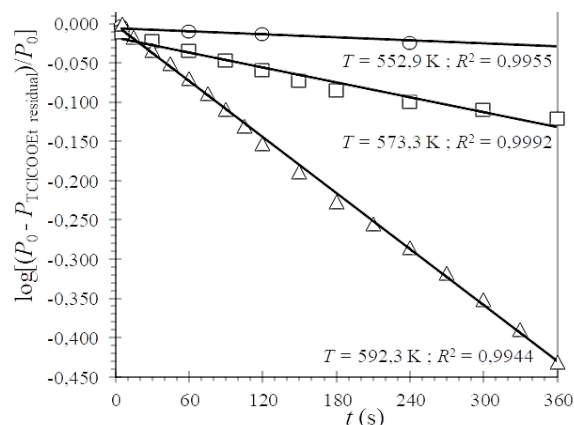

Figure 7. First-order graph for ethyl chlorooxoacetate thermolysis.

The values of the rate coefficient were obtained from the following equation:

$$k_1 = -(2{,}303/t)\log[(P_0 - P_{ClCOOEt})/P_0] \quad (7)$$

Inhibitor effect. In order to prevent the reaction from following a free radical chain mechanism [14-18], instead of using the molecular route, toluene was utilized as radical inhibitor [20-25] in different proportions. It can be observed in Table 3 how the invariability of the rate coefficient in the presence and absence of toluene indicates that the reaction under study was not inhibited, which suggests a molecular mechanism.

Table 3. Effect of toluene as inhibitor on rate coefficient in ethyl chlorooxoacetate thermolysis at 582.5 K.

Inhibitor pressure, P_i (mbar)	Initial pressure, P_0 (mbar)	Relation P_i/P_0	$10^4 k_1$ (s⁻¹)	Average $\langle 10^4 k_1\rangle$ (s⁻¹)	DSR (%)
	111.99	–	7.10		
119.99	98.66	1.22	6.97	6.99 ± 0.09	1.29
183.32	93.33	1.96	6.88		
258.65	83.99	3.08	6.99		

Homogeneity. In order to verify that thermolysis occurred quantitatively in gas phase [26-28], it was additionally carried out in a reactor internally packed with small Pyrex glass cylinders with a surface-area-to-volume ratio of 6.22 cm⁻¹ (Figure 8), assuming a 1:1 ratio in the unpacked reactor (Figure 4). The findings were only consistent when both reactors were internally covered with a layer of the carbon produced in allyl bromide thermolysis at above 673 K [29]. It was not possible to obtain reproducible results in reactors with no carbon coating, which reveals that the nature of the glass surface can significantly affect the reaction rate [30].
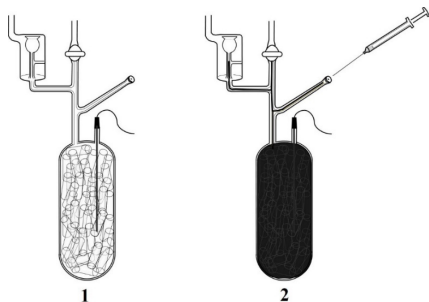

Figure 8. Packed Pyrex glass reactor: 1, clean. 2, coated with carbon in thermolysis at 673 K after injecting allyl bromide.

The findings indicate that the reaction is homogeneous under such conditions.

Table 4. Homogeneity in ethyl chlorooxoacetate thermal decomposition at 573.2 K.

$10^4 k_1$ (s⁻¹)	
Unpacked reactor (SA:V = 1 cm⁻¹)	Packed reactor (SA:V = 6.22 cm⁻¹)
7.05 ± 0.16	7.70 ± 0.38

Temperature Effect

The kinetic parameters were determined by linear regression of the results in Table 5 and Figure 9, which also corresponds to Arrhenius plot.

Table 5. Arrhenius plot values for ethyl chlorooxoacetate thermolysis.

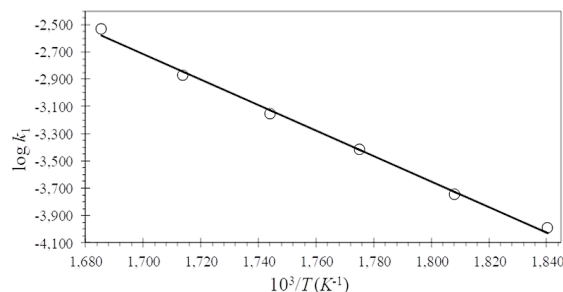| T (K)	543.2	552.9	563.2	573.2	583.3	593.1
$10^4 k_1$ (s⁻¹)	1.01	1.80	3.82	7.00	13.47	29.36

Figure 9. Influence of temperature on ethyl chlorooxoacetate reaction rate coefficient. Slope: − (9371.9 ± 256.0) K. Intercept: (13.22 ± 0.45). R^2 = 0.9990 ± 0.0333. Confidence level: 90%

Thus, the Arrhenius equation was obtained for the reaction between 543.2 – 593.1 K:

$$\log k_1(\text{s}^{-1}) = (13.22 \pm 0.45) - (179.4 \pm 4.9)\,\text{kJ mol}^{-1}(2.303\,RT)^{-1} \quad (8)$$

Based on the transition state theory, it is possible to determine the kinetic and activation thermodynamic parameters, through the following equations for unimolecular reactions:

$$\Delta G^{\neq} = \Delta H^{\neq} - T\Delta S^{\neq} \quad (9)$$

$$\Delta H^{\neq} = E_a - RT \quad (10)$$

$$\Delta S^{\neq} = R \ln\left(\frac{A\,h}{e\,k_{\mathrm{B}}\,T}\right) \qquad (11)$$

The results obtained by extrapolation at 623 K are presented in Table 6. This temperature was chosen to be able to include the results of ethyl oxoacetate decarbonylation, in order to discuss the effect of the substituent to carbonyl group on reactivity.

Table 6. Comparison between the kinetic parameters obtained at 623 K in the ethyl oxoacetate decarbonylation and ethyl chlorooxoacetate reactions.

Z^a	$10^4 k_1$ (s^{-1})	$\log A$	E_a (kJ mol^{-1})	$\Delta H^{\neq}$ (kJ mol^{-1})	$\Delta S^{\neq}$ (J mol^{-1}K^{-1})	$\Delta G^{\neq}$ (kJ mol^{-1})	Ref.
Cl	151.57	13.22 ± 0.45	179.4 ± 4.9	227.7	-6.3	178.1	b
H	0.034	14.06 ± 0.54	232.9 ± 7.0	174.2	9.8	22.6	9

^{a}Substituent in the acylic part of the ester

^{b}This study

In light of these results, a mechanism involving decarbonylation and ethylene elimination is suggested. In this case, consecutive reactions occur, in contrast to ethyl oxoacetate thermolysis, in which parallel reactions take place.
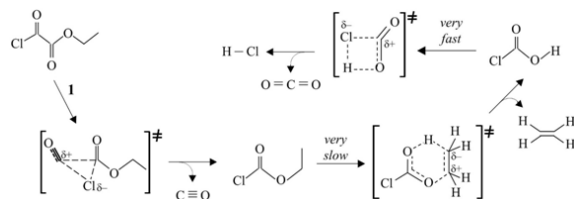

Figure 10. Mecanism for ethyl chlorooxoacetate thermal decomposition.

In both cases, positive values of enthalpy and activation free energy suggest endothermic and endergonic transition states. The negative value of activation entropy in ethyl chlorooxoacetate decarboxylation can be attributed to the formation of a triple bond in the transition state, which decreases the degrees of freedom. This contrasts with the ethyl oxoacetate decarbonylation reaction, whose positive activation entropy can be due to the fact that the acylic hydrogen may form less rigid bonds in the transition state given its acid/nucleophile dual behavior. The chlorine substituent seems to assist the decarbonylation reaction over the elimination reaction. This behavior can be explained in terms of electronic transmission: the chlorine atom is a good "leaving" atom and has non-bonding electronic pairs. These properties allow it to migrate and attack nucleophilically the positive

charge density generated in the carbon atom of its neighbor carbonyl group in transition state. This behavior suggests that the more electronegative the substituent is, the higher its tendency to migrate to its neighbor carbonyl will be, since it tends to attract the electronic density of its neighbor carbonyl as the bond of the adjacent carbonyl groups is weakened in transition state, as shown in Figure 10. This comes to explain the fact that the rate coefficient of ethyl chlorooxoacetate decarbonylation is dramatically higher than in ethyl oxoacetate.

Conclusions

In view of the qualitative-quantitative analysis of products and kinetic parameters obtained, it is possible to propose a decarbonylation mechanism, with consecutive decarboxylation and ethylene elimination reactions, for the unimolecular and homogeneous elimination of ethyl chlorooxoacetate. Ethyl chlorooxoacetate activation entropy is negative because chlorine has a salient tendency to migrate to its neighbour carbonyle, forming bonds with fewer degrees of freedom in the transition state. The tendency displayed by a substituent to migrate to the adjacent carbonyl group in decarbonylation reactions seems to be directly proportional to its electronegativity. At the same temperature, the ethyl chlorooxoacetate decarbonylation reaction was superior to ethyl oxoacetate decarbonylation over three magnitude orders.

Acknowledgement

References

[1]   Chuchani G., Martin I. & Avila I. "Effect of substituents in the gas-phase elimination kinetics of β-substituted ethyl acetates". Int. J. Chem. Kinet., Vol 11, Nº 6 (1979) 561-567. https://doi.org/10.1002/kin.550110602

[2]   Al-Awadi N.A., Kaul K. & El-Dusouqui O.M. "Kinetics and mechanism of thermal gas-phase elimination of α-substituted carboxylic acids: role of relative basicity of α-substituents and acidity of incipient proton". J. Phys. Org. Chem., Vol 13, Nº 9 (2000) 499-504. https://doi.org/10.1002/1099-1395(200009)13:9<499::AID-POC269>3.0.CO;2-0

[3]   Al-Awadi S.A., Abdallah M.R., Dib H.H., Ibrahim M.R., Al-Awadi N.A. & El-Dusouqui O.M.E. "Kinetics and mechanism of thermal gas-phase elimination of β-substituted carboxylic acids". Tetrahedron, Vol. 61, Nº 24 (2005), 5769-5777. https://doi.

org/10.1016/j.tet.2005.04.031

[4]   Silva A.M. "A theoretical study of the pyrolysis of isopropyl acetate". Chem. Phys. Lett., Vol. 439, Nº 1-3 (2007) 8-13. https://doi.org/10.1016/j.cplett.2007.03.037

[5]   Floyd K. & Smith G. "Structure-reactivity relationships in homogeneous gas phase reactions: thermolysis and rearrangements". Prog. Phys. Org. Chem., Vol. 8 (2009) 75. https://10.1002/9780470171875.ch2

[6]   Moldoveanu S.C. "The chemistry of the pyrolytic process". In Techniques and Instrumentation in Analytical Chemistry, Amsterdam, Elsevier, Vol 28 (2010) 28:7-48. https://doi.org/10.1016/S0167-9244(09)02802-9

[7]   Wu P., Chen X., Li J. & Huang Y. "Theoretical studies on the pyrolysis of thiocarbonates". Comput. Theor. Chem., Vol. 1030 (2014) 67-73. https://doi.org/10.1016/j.comptc.2013.12.026

[8]   Shiroudi A. & Zahedi E. "Understanding the kinetics of thermal decomposition of 2, 3-epoxy-2, 3-dimethylbutane using RRKM theory". RSC Adv., Vol. 6, Nº 94 (2016) 91882-91892. https://doi.org/10.1039/C6RA21963B

[9]   Al-Awadi N. "Gas Phase Pyrolytic Reactions. Chapter 4: Structure/Reactivity Correlation" (2019) https://doi.org/10.1002/9781119010753.ch4

[10]   Laidler K.J. "Reaction kinetics: Homogeneous gas reactions". Vol. 1. Amsterdam, Elsevier (2013) 97-149.

[11]   Cordova T., Rotinov A. & Chuchani G. "Experimental and theoretical study of the homogeneous, unimolecular gas-phase elimination kinetics of methyl oxalyl chloride". J. Phys. Org. Chem. Vol 17, Nº 2 (2004) 148-151. https://doi.org/10.1002/poc.705

[12]   Reyes Y.A. "Estudio cinético de la termólisis del oxoacetato de etilo". Afinidad, Vol. 74, Nº 579 (2017) 208-213. https://www.raco.cat/index.php/afinidad/article/view/328556

[13]   Johnson R. L. & Stimson V.R. "The thermal decomposition of ethyl chloroformate". Aust. J. Chem., Vol. 29, Nº 6 (1976) 1389-1392. https://doi.org/10.1071/CH9761389

[14]   Benson, S.W. "Predictability of chain reactions". Ind. Eng. Chem., Vol. 56, Nº 1 (1964) 18-27. https://doi.org/10.1021/ie50649a004

[15]   Márquez E., Domínguez R., Tosta M. & Chuchani, G. "Cinética y mecanismos de la eliminación homogénea en fase gaseosa unimolecular del ortoacetato de trimetilo y del ortobutirato de trimetilo". J. Phys. Chem. A, Vol. 112, Nº 47 (2008) 12140-12142. https://doi.org/10.1021/jp8074942

[16]   Vasiliou A.G., Piech K.M., Zhang X., Nimlos M.R., Ahmed M., Golan A. et al. "The products of the thermal decomposition of CH3CHO". J. Chem. Phys., Vol. 131, Nº 1 (2011) 014306. https://doi.org/10.1063/1.3604005

[17]   Moreno B.M, Quach A.L., Merves M.N. & Klein M.T. "Discrimination between free-radical and concerted pyrolysis mechanisms". Energy Fuels, Vol. 28, Nº 7 (2014) 4256-4259. https://doi.org/10.1021/ef500055a

[18]   Trubetskaya A., Jensen P.A., Jensen A.D., Glarborg P., Larsen F.H. & Andersen M.L. "Characterization of free radicals by electron spin resonance spectroscopy in biochars from pyrolysis at high heating rates and at high temperatures". Biomass Bioenergy, Vol. 94 (2016) 117-129. https://doi.org/10.1016/j.biombioe.2016.08.020

[19]   Vahid S. & Zokaie M. "Multichannel Gas-Phase Unimolecular Decomposition of Acetone: Theoretical Kinetic Studies". J. Phys. Chem. A, Vol. 122, Nº 28 (2018) 5895-5904. https://doi.org/10.1021/acs.jpca.8b02423

[20]   Colket M.B. & Seery D.J. (1994, January). "Reaction mechanisms for toluene pyrolysis". In Symposium (International) on combustion (Vol. 25, No. 1, pp. 883-891). Elsevier. https://doi.org/10.1016/S0082-0784(06)80723-X

[21]   Sivaramakrishnan R., Tranter R.S. & Brezinsky K. "High pressure pyrolysis of toluene. 1. Experiments and modeling of toluene decomposition". J. Phys. Chem A., Vol. 110, Nº 30 (2006) 9388-9399. https://doi.org/10.1021/jp060820j

[22]   Sivaramakrishnan R., Tranter R.S. & Brezinsky K. "High pressure pyrolysis of toluene. 2. Modeling benzyl decomposition and formation of soot precursors". J. Phys. Chem. A, Vol. 110, Nº 30 (2006) 9400-9404. https://10.1021/jp0608224

[24]   Zhang L., Cai J., Zhang T. & Qi F. "Kinetic modeling study of toluene pyrolysis at low pressure". Combust. Flame, Vol. 157, Nº 9 (2010) 1686-1697. https://10.1016/j.combustflame.2010.04.002

[24]   Lannuzel F., Bounaceur R., Michels R., Scacchi G. & Marquaire P.M. "An extended mechanism including

high pressure conditions (700bar) for toluene pyrolysis". J. Anal. Appl. Pyrol., Vol. 87, Nº 2 (2010) 236-247. https://10.1016/j.jaap.2010.01.001

[25]   Matsugi A. & Miyoshi A. "Modeling of two- and three-ring aromatics formation in the pyrolysis of toluene". Proc. Comb. Inst., Vol. 31, Nº 1 (2013) 269-277. https://10.1016/j.proci.2012.06.032

[26]   Taylor J.E. & Milazzo T.S. "Gas-phase pyrolysis of 2,2,3,3-tetramethylbutane using a wall-less reactor". Int. J. Chem. Kinet., Vol. 10, Nº 12 (1978) 1245-1257. https://doi.org/10.1002/kin.550101207

[27]   Dabbagh H.A. & Davis B.H. "Pyrolysis of sec-butyl acetate. Is the stereospecific syn elimination a homogeneous or heterogeneous reaction? J. Org. Chem., Vol. 55, Nº 7 (1990) 2011-2016. https://doi.org/10.1021/jo00294a011

[28]   Mascavage L.M. & Dalton D.R. "Surface catalyzed hydrochlorination of 1,3-butadiene". Tetrahedron Lett., Vol. 32, Nº 29 (1991) 3461-3464. https://doi.org/10.1016/0040-4039(91)80806-H

[29]   Maccoll A. "Studies in the pyrolysis of organic bromides. Part I. The kinetics of the decomposition of allyl bromide". J. Chem. Soc. (1955) 965-973. https://doi.org/10.1039/JR9550000965

[30]   Acevedo S., Galicia L., Plaza E., Atencio R., Rodríguez A. & González E. "Carbón activado preparado a partir de carbón mineral bituminoso activado con hidróxido de potasio". Rev. Téc. Ing. Univ. Zulia. Vol. 39, No 2 (2016) 64-70. https://www.produccioncientificaluz.org/index.php/tecnica/article/view/21324